Published in final edited form as:
Cell. 2014 January 30; 156(3): 522–536. doi:10.1016/j.cell.2013.12.040.

Control of stress-induced persistent anxiety by an extra-amygdala septohypothalamic circuit

Todd E. Anthony[1], **Nick Dee**[2], **Amy Bernard**[2], **Walter Lerchner**[1,3], **Nathaniel Heintz**[4,5], and **David J. Anderson**[1,5]

[1]California Institute of Technology, Division of Biology, 1200 East California Blvd, M/C 156-29, Pasadena, CA 91125

[2]Allen Institute for Brain Science, 551 North 34th St, Suite 200, Seattle, WA 98103

[4]The Rockefeller University, 1230 York Avenue, New York, NY 10021

[5]Howard Hughes Medical Institute

Abstract

The extended amygdala has dominated research on the neural circuitry of fear and anxiety, but the septo-hippocampal axis plays an important role as well. The lateral septum (LS) is thought to suppress fear and anxiety, through its outputs to the hypothalamus. However, this structure has not yet been dissected using modern tools. The type 2 CRF receptor (*Crfr2*) marks a subset of LS neurons, whose functional connectivity we have investigated using optogenetics. *Crfr2*$^+$ cells include GABAergic projection neurons that connect with the anterior hypothalamus. Surprisingly, we find that these LS outputs enhance stress-induced behavioral measures of anxiety. Furthermore, transient activation of *Crfr2*$^+$ neurons promotes, while inhibition suppresses, persistent anxious behaviors. LS *Crfr2*$^+$ outputs also positively regulate circulating corticosteroid levels. These data identify a subset of LS projection neurons that promote, rather than suppress, stress-induced behavioral and endocrinological dimensions of persistent anxiety states, and provide a cellular point-of-entry to LS circuitry.

INTRODUCTION

Stress is an etiologic factor in psychiatric disorders, especially those involving anxiety (Gross and Hen, 2004; Feder et al., 2009; Lupien et al., 2009). Consequently, considerable effort has been made to map the neural circuits through which stress promotes anxiety, most recently using optogenetic tools (Nieh et al., 2012; Tye and Deisseroth, 2012). The majority of such studies have focused on the extended amygdala (EA)(Davis et al., 2010; Tye et al., 2011; Mahan and Ressler, 2012; Jennings et al., 2013; Kim et al., 2013). The septo-hippocampal axis (SHA) has also been implicated (Gray and McNaughton, 2000), but has received less attention in the modern era. Several studies have indicated a role for the ventral hippocampus in anxiety (Henke, 1990; Kjelstrup et al., 2002; Felix-Ortiz et al., 2013;

[3]Current address: National Institutes of Health, Bethesda, MD 20892

SUPPLEMENTAL INFORMATION

Supplemental Experimental Procedures and figures and can be found with this article online.

Kheirbek et al., 2013). However, the lateral septum (LS), a major component of the SHA (Fig. 1B), has been relatively neglected in comparison to the intense focus on the EA.

The LS receives topographically organized inputs from the hippocampus (Risold and Swanson, 1996) and is in turn reciprocally connected with the hypothalamus (Risold and Swanson, 1997b) (Fig. 1A). It is also cellularly heterogeneous (Risold and Swanson, 1997a). A variety of stressors induce immediate early gene (IEG) expression in subsets of LS neurons (reviewed in (Sheehan et al., 2004)). Furtherore, traumatic stress triggers a persistent enhancement of LS IEG induction in response to innately aversive stimuli (Mongeau et al., 2003). Importantly, whether such stress-induced activation of the LS serves to promote, or rather to inhibit, persistent anxiety states is not clear.

Classical lesions of the septum, including both its medial and lateral subdivisions, resulted in the dramatic 'septal rage' phenotype, characterized by exaggerated defensive responses to non-threatening stimuli (Spiegel et al., 1940; Brady and Nauta, 1953). Reversible inactivation of the LS yielded similar phenotypes (Albert and Richmond, 1976; Albert and Wong, 1978). These and other data have led to a prevailing view that LS output is anxiolytic, i.e., dampens fear or anxiety (reviewed in (Sparks and LeDoux, 2000; Sheehan et al., 2004)).

Other studies, however, have implied an anxiogenic role for the LS (Drugan et al., 1986; Treit and Pesold, 1990). For example, LS injections of agonists of the type 2 corticotropin-releasing factor receptor (*Crfr2*) have resulted in increased anxiety (Radulovic et al., 1999; Bakshi et al., 2002; Henry et al., 2006). However, it is not clear whether such agonists excite or inhibit the neurons that express these receptors (Liu et al., 2004; Liu et al., 2005). Indeed, *Crfr2* mutations increase anxiety, implying an anxiolytic function for the receptor (Bale and Vale, 2004). These ambiguities, together with the unknown anatomy and connectivity of *Crfr2*$^+$ neurons, preclude any inferences of functional LS circuitry to be made from such pharmacologic and genetic data (Fig. 1C, D).

As an initial step towards dissecting the circuitry through which the LS regulates anxiety, we have gained genetic access to *Crfr2*-expressing neurons, and have used optogenetics, electrophysiology and anatomical mapping to understand how the electrical activity of these neurons influences anxiety, and the connectivity through which this influence is exerted. We find, contrary to the prevailing view, that *Crfr2* marks LS output neurons whose activity promotes, rather than inhibits, anxiety, in a persistent manner. Thus LS output does not serve exclusively to suppress fear or anxiety in response to stressors (Sheehan et al., 2004).

RESULTS

Crfr2 expression identifies a subset of GABAergic LS neurons

In situ hybridization (ISH) revealed that *Crfr2* mRNA is expressed by a subset of LS cells (Figs. 2A–E). Double fluorescence ISH (dFISH) revealed that most *Crfr2*$^+$ cells express the GABA biosynthetic gene *Gad2* (1,765/2,076 = 85.0%; Fig. 2F), whereas no overlap was detected with either glutamatergic or cholinergic markers (Fig. S1), indicating that *Crfr2* is expressed primarily by GABAergic neurons. Comparison of *Crfr2* mRNA to that of *Esr1* or *Penk*, two genes heterogeneously expressed in the LS (Risold and Swanson, 1997a) indicated little or no overlap at the single cell level: *Crfr2* vs. *Esr1*, *Crfr2*$^+$/DAPI$^+$ = 8.3%, *Esr1*$^+$/DAPI$^+$ = 1.7%; 8.3%×1.7%×11,086 cells counted = 15 *Crfr2*$^+$*Esr1*$^+$ cells expected if expression were random; 0 *Crfr2*$^+$*Esr1*$^+$ cells were observed; *Crfr2* vs. *Penk*, *Crfr2*$^+$/DAPI$^+$ = 9.3%, *Penk*$^+$/DAPI$^+$ = 3.3%; 9.3%×3.3%×8,274 cells counted = 25 *Crfr2*$^+$*/Penk*$^+$ cells expected if expression were random; 1 *Crfr2*$^+$*Penk*$^+$ cell was observed (Figs. 2G–J). These

data indicate that *Crfr2*$^+$ neurons are distinct from other molecularly defined populations of LS cells.

To enable genetic manipulation of *Crfr2*$^+$ neurons, we generated BAC (bacterial artificial chromosome) transgenic mice expressing an eGFPCre fusion protein (Gagneten et al., 1997)) under the control of the brain-selective alpha splice variant of the *Crfr2* gene (Fig. 2K). Comparison by dFISH of eGFPCre expression to that of endogenous *Crfr2* mRNA indicated that 86.6% of Cre$^+$ cells contained *Crfr2* mRNA; conversely, 34.4% of *Crfr2 mRNA*$^+$ cells were Cre$^+$ (Figs. 2L,M). This indicates that the BAC transgene is highly specific for *Crfr2*$^+$ neurons, but may be expressed in a subset of such cells. Immunostaining revealed that many eGFPCre$^+$ cells are surrounded by pericellular baskets containing UCN3, a CRFR2 peptide ligand (Figs. 2N,O), suggesting that these cells respond to this ligand in vivo.

To examine Cre-mediated recombination in *Crfr2α*-eGFPCre mice, the LS was injected with a Cre-dependent (FLEx) adeno-associated virus (AAV) encoding membrane-targeted tdTomato reporter (channelrhodopsin-2 (ChR2)-tdTomato(tdT) fusion) (Atasoy et al., 2008) (Fig. 2P). Almost 80% (77.9%) of tdT$^+$ cells contained detectable eGFPCre$^+$ nuclei (Figs. 2Q,R). The presence of tdT in some eGFPCre$^-$ cells may reflect low and/or transient expression of Cre, coupled with the high sensitivity and perdurance of fluorescent marker expression, as observed in other Cre driver lines (Madisen et al., 2010). In support of this idea, dFISH showed that 91.6% of tdT mRNA$^+$ cells were *Crfr2* mRNA$^+$ (Figs. 2S,T). Importantly, recombination did not occur in ESR1$^+$ or *Penk*$^+$ LS neurons (Fig. S2). Thus, the *Crfr2α*-eGFPCre BAC transgene restricts recombination of injected Cre-dependent viruses to LS *Crfr2*$^+$ neurons.

Optogenetic activation of *Crfr2α*$^+$ neurons is anxiogenic

The valence of LS *Crfr2α*$^+$ neuronal activity with respect to anxiety is unclear. Although infusions of CRFR2 receptor agonists into LS have consistently yielded anxiogenic effects (Radulovic et al., 1999; Bakshi et al., 2002; Henry et al., 2006; Bakshi et al., 2007), slice recordings showed that receptor activation can both inhibit (Liu et al., 2004) and potentiate (Liu et al., 2005) neuronal activity. Consequently, it is unknown whether CRFR2 receptor activation increases anxiety through a decrease or an increase in *Crfr2α*$^+$ neuronal activity (Figs. 1C,D). Therefore we tested whether direct activation of *Crfr2α*-expressing neurons increases or decreases anxiety.

To do this, we targeted a Channelrhodopsin-2-yellow fluorescent protein fusion (ChR2-YFP) to *Crfr2α*$^+$ neurons by injecting a Cre-dependent AAV (Fig. 3A) into the LS of *Crfr2α*-eGFPCre mice. ChR2-YFP was spatially correlated with Cre expression and restricted to the LS, with no ChR2-YFP$^+$ cell bodies detected outside of this region (Figs. 3B–E and data not shown). Slice recordings revealed that ChR2-YFP$^+$ neurons could be efficiently and repetitively photostimulated at rates up to 15 Hz (Figs. 3F–H and Figs. S3A–C). Although LS *Crfr2*α$^+$ neuron in vivo firing rates are unknown, single unit recordings in the LS have observed spike frequencies as high as 26 Hz (Thomas et al., 2005). Furthermore, LS recordings during elevated plus maze (EPM) tests identified units whose activity increased from ~7.5 Hz in the closed arms to ~12.5 Hz in the open arms (Thomas et al., 2013). We therefore chose a photostimulation rate of 15 Hz, which is in the range of natural firing rates of LS neurons in anxiogenic environments.

Three behavioral tests of anxiety were used: light-dark box (LDB), open field (OF), and novel object (NO)(Figs. 3I,J); these tests were chosen as pharmacological experiments showed them to be sensitive to modulation of LS *Crfr2*$^+$ neuronal function (Henry et al., 2006). Photostimulation during testing significantly increased anxiety levels in the ChR2

group in all three assays relative to light-stimulated control animals injected with Cre-dependent AAV encoding hrGFP (Fig. 3K). Anxiogenic effects were also detected in the EPM (Fig. S3D). These effects were not due to a change in locomotor activity (Fig. S3E). In the absence of light, no significant differences were detected (Fig. S3F). Thus, direct optogenetic stimulation of *Crfr2α*$^+$ neurons during behavioral testing increases anxiety (Fig. 3N).

Transient activation of *Crfr2α*$^+$ neurons causes a persistent state of anxiety

One feature of anxiety states is their persistence. Therefore, we tested whether transient optogenetic stimulation of *Crfr2α*$^+$ neurons might cause persistent anxiogenic effects. Pharmacological approaches, such as injection of CRFR2 agonists, cannot address this issue since once a drug is infused, the duration of its action is unknown.

Mice subjected to 30 minutes of photostimulation were subsequently transferred to a separate room and behaviorally assayed in the absence of photostimulation (Figs. 3J,L). ChR2-expressing mice showed increased levels of anxiety relative to eYFP controls throughout the 35 minute testing period (Fig. 3L) without differences in locomotor behavior (Fig. S3G). Re-testing of these mice 7 days later in the absence of additional photostimulation yielded no significant differences in anxiety behavior (Fig. S3H), indicating that the anxious state induced by *Crfr2α*$^+$ neuronal stimulation is reversible. Furthermore, photostimulation at 1 Hz did not produce significant increases in anxiety (Fig. S3I), suggesting that the persistent effect of activating *Crfr2α*$^+$ neurons is frequency-dependent.

The severity of a stressful encounter is thought to influence the degree of its anxiogenic consequences (Adamec et al., 2006). We therefore asked whether photostimulation of LS *Crfr2α*$^+$ neurons can exacerbate the anxiogenic effects of immobilization stress (IMS). Mice were subjected to IMS for 30′, throughout which time they received photostimulation. During subsequent testing done in a separate room in the absence of photostimulation, ChR2 mice showed higher levels of anxiety behavior than controls, indicating that stimulation of LS *Crfr2α*$^+$ neurons and IMS can combine to exacerbate anxiety (Fig. 3M).

Crfr2α$^+$ neuronal activity is necessary for the induction and expression of a stress-induced, sensitized state

The foregoing experiments indicated that stimulation of *Crfr2α*$^+$ neurons is sufficient to increase anxiety in a persistent manner, but did not address whether the activity of these neurons is normally required for stress-induced anxiety. In principle, *Crfr2α*$^+$ neuronal activity could be necessary for the induction or maintenance (or both) of a persistent anxious state. To distinguish these possibilities, we injected *Crfr2α*-eGFPCre mice with a Cre-dependent AAV (Fig. 4A) encoding yellow fluorescent protein (YFP) fused to the enhanced halorhodopsin from Natronomonas pharaonis (eNpHR2.0), a light-driven chloride pump that hyperpolarizes neurons in response to yellow light (Gradinaru et al., 2008). A crescent-shaped pattern of eNpHR-YFP protein was observed that was restricted to LS and correlated closely with Cre$^+$ cells (Figs. 4B–E and data not shown). Slice recordings confirmed that yellow light produced outward currents that hyperpolarized eNpHR-YFP$^+$ neurons without detectable rebound firing even after prolonged, repeated photoinhibition (Figs. S4A–D), and that were sufficient to suppress current injection-induced firing (Figs. 4F–H).

To induce an anxious state, mice were subjected to 20′ of IMS after which they were transferred to the testing room and behaviorally assayed (Figs. 4I,J). To ascertain the temporal roles of *Crfr2α*$^+$ neurons, the LS was illuminated with 593nm light either during IMS or subsequent testing. Photoinhibition of *Crfr2α*$^+$ neurons produced significant

anxiolytic effects in eNpHR-injected mice relative to hrGFP controls, regardless of whether inhibition was done during IMS or testing (Figs. 4L,K). No differences in locomotor behavior were observed (Figs. S4E,F). In the absence of 593nm light, no differences were observed between groups (Fig. S4H). Comparisons of light ON vs. OFF periods indicated that the anxiolytic effects were predominant during illumination, and therefore unlikely to be due to rebound firing following photoinhibition offset (Fig. S4G).

One caveat was the possibility that the testing environment itself is highly stressful. If so, then the anxiolytic effects of inhibition during testing (Fig. 4L) might reflect a role for *Crfr2a*$^+$ neurons in responding to the stress of the testing conditions, rather than in the expression of a previously established sensitized state. However, no significant reduction in anxiety was observed when photoinhibition of *Crfr2a*$^+$ neurons was done during testing in mice that had not undergone IMS (Fig. 4M). These data suggest that ongoing activity of *Crfr2a*$^+$ neurons is required for both the induction and persistence of a stress-induced anxious state (Fig. 4N). Taken together, our gain- and loss-of-function data indicate that the activity of *Crfr2a*$^+$ neurons exerts a net anxiogenic influence (Fig. 1C).

LS *Crfr2a*$^+$ GABAergic projections to the anterior hypothalamus mediate persistent stress-induced anxiety

It is not known whether LS *Crfr2a*$^+$ neurons are interneurons or projection neurons, nor have their synaptic targets been identified. Therefore, their anxiogenic influence could reflect either a local, intra-septal (interneuron) or extra-septal (projection neuron) function (Fig. 1, C1 vs. C2). To determine whether LS *Crfr2a*$^+$ neurons have extra-septal projections, ChR2-YFP was used as an anterograde label (Fig. 5A). Strong somatodendritic labeling of neurons was observed, as was a robust projection of YFP$^+$ axons coursing ventrally out of the LS (Figs. 5B–D). The extra-septal region containing the densest cluster of axons was the anterior hypothalamic area (AHA) of the medial hypothalamus (Figs. 5E,F), with lighter innervation seen in more rostral and caudal hypothalamic areas, medial amygdala, periaqueductal gray, and ventral hippocampus (Figures S5A–L). Notably, the paraventricular nucleus (PVN), which is part of the hypothalamic-pituitary-adrenocortical (HPA) axis (reviewed in (Ulrich-Lai and Herman, 2009)), appeared to exclude *Crfr2a*$^+$ axons (Fig. 5G).

To further characterize these putative long range targets of *Crfr2a*$^+$ neurons, we iontophoresed cholera toxin subunit B (CTB) into the AHA of *Crfr2a*-eGFPCre mice (Fig. 5H). At middle coronal levels of LS (bregma+0.6), back labeled neurons formed a crescent pattern that overlapped with *Crfr2a*$^+$eGFPCre$^+$ cell bodies (Figs. 5I,J). Moreover, the overlap of eGFPCre and CTB at the single cell level was significantly higher than that expected by chance (Fig. 5K). In contrast, significantly fewer *Crfr2a*$^+$eGFPCre$^+$ neurons were labeled than that expected by chance when CTB was iontophoresed into the lateral hypothalamus (LH, a known target of LS innervation (Risold and Swanson, 1997b; Sartor and Aston-Jones, 2012)), despite similar numbers of back-labeled LS cells (Figs. 5L–O). These data suggest that *Crfr2a*-expressing cells at middle levels (bregma+0.6) of LS preferentially project to AHA vs. LH.

To determine the postsynaptic effects of stimulating *Crfr2a*$^+$ axons, we employed Channelrhodopsin-2 (ChR2)-assisted circuit mapping (CRACM) (Petreanu et al., 2007) to assay postsynaptic responses in AHA neurons near ChR2-YFP$^+$ axons (Fig. 5P). In 6/9 cells tested, 473nm light evoked picrotoxin-sensitive inhibitory postsynaptic currents (IPSCs) (average amplitude = 71.3±5.3pA) (Fig. 5Q, top). Responses occurred with a latency of 5.0±0.4 ms, consistent with monosynaptic connectivity (Debanne et al., 2008). Moreover, photostimulation was sufficient to inhibit spiking in postsynaptic cells (Fig. 5Q, bottom). Similar results were obtained from local intra-septal targets of *Crfr2a*$^+$-ChR2-expressing

neurons in LS slice recordings (Figs. S5M,N). Thus, LS *Crfr2α*$^+$ projection neurons form inhibitory synapses with target neurons in the AHA. Neurons in this population also make local inhibitory synapses within the LS. Whether these local and long-range synapses are made by the same or different *Crfr2α*$^+$ neurons is not clear.

The existence of projections to AHA does not in itself establish a role for these connections in the anxiogenic influence of *Crfr2α*$^+$ neuronal activity, since it remained possible that such effects are mediated principally via local intra-septal synapses. To test the requirement of projections to the AHA for the expression of stress-induced anxiety, we employed the archaerhodopsin ArchT, a light-driven proton pump that hyperpolarizes neurons in response to green light and efficiently traffics to axonal termini (Han et al., 2011). Injection of a Cre-dependent AAV (Fig. 6A) into *Crfr2α*-eGFPCre LS yielded ArchT expression in a pattern that correlated with Cre and enabled photoinhibition of cell bodies and axons (Figs. S6B–M).

Photoinhibition of LS *Crfr2α*$^+$ terminal fields in the AHA during behavioral testing following IMS produced significant anxiolytic effects without altering locomotor behavior, and no significant differences were observed in the absence of 532nm light (Figs. 6B–E and S6N,O). Conversely, optogenetic stimulation using ChR2-YFP of LS *Crfr2α*$^+$ axon terminals in the AHA during testing was anxiogenic in the LDB and OF assays, albeit more weakly than was observed using LS cell body stimulation (Figs. 6F–J); locomotor behavior was unaffected (Fig. S6P). Antidromic stimulation of LS cell bodies may contribute to the behavioral effects of optogenetic terminal activation, but cannot be exclusively responsible given that photoinhibition of terminals in this region using ArchT was anxiolytic (Fig. 6E). Together these data suggest that LS *Crfr2α*$^+$ neurons exert anxiogenic effects, at least in part, via inhibitory projections to the AHA (Fig. 1C2).

LS *Crfr2α*$^+$ neurons make di-synaptic connections with PVN via AHA

Despite strong innervation by LS *Crfr2*α$^+$ axons of the adjacent AHA, the PVN appears devoid of such projections (Fig. 5G). Given the role of the PVN in the stress response, we asked whether the PVN might be a higher-order target of LS *Crfr2*α$^+$ neurons. To test for evidence of polysynaptic connectivity, we used the herpes simplex virus (HSV) strain HSV129ΔTK-TT (Fig. 7A), a Cre-dependent transneuronal tracer that moves exclusively in the anterograde direction (Lo and Anderson, 2011).

At 1 day following delivery of the virus into the LS of *Crfr2α*-eGFPCre mice, scattered tdT$^+$ cells were observed near the injection site (Fig. 7B) but not in any other region. By 3 days post-injection, tdT labeling was extensive throughout the LS on the side ipsilateral to injection (Fig. 7C), and many tdT$^+$ cells were now detectable bilaterally in both the AHA and PVN (Fig. 7D), consistent with di- or poly-synaptic transfer to the latter structure. Many tracer-labeled AHA neurons were GABAergic (Fig. S7E–H). The anterogradely labeled dorsolateral PVN cells were located in a region known to contain parvicellular CRF$^+$ neurons of the mouse PVN that are responsible for initiating the stress responses (Biag et al., 2012). No tdT fluorescence was detected when HSV129ΔTK-TT was injected into the LS of nontransgenic animals (data not shown).

To test whether LS *Crfr2α*$^+$ neurons monosynaptically inhibit AHA neurons that innervate the PVN, *Crfr2*α-eGFPCre mice were co-injected in the LS with Cre-dependent ChR2-YFP, and in the PVN with retrobeads (RB, retrograde tracer) (Figs. 7E,F). Recordings of RB$^+$ cells in the AHA identified 4/9 cells that showed monosynaptic IPSCs in response to a 2ms pulse of 473nm light (average amplitude = 74.6±33.4pA; average latency = 5.5±0.1 ms) and that were sufficient to inhibit firing (Fig. 7G). Taken together with the results of the HSV129ΔTK-TT anterograde tracing, these data demonstrate that LS *Crfr2α*$^+$ neurons make

di-synaptic connections to the PVN via their projections to the AHA. Similar experiments indicated that LS *Crfr2α*$^+$ neurons also form inhibitory synapses on AHA neurons that project to the midbrain periaqueductal gray (PAG; Figure S7I–L), a region known to regulate defensive behaviors relevant to anxiety (Bandler and Shipley, 1994; Almeida-Santos et al., 2013).

AHA-projecting LS *Crfr2α*$^+$ neurons positively regulate corticosterone levels

The PVN is innervated by GABAergic AHA neurons implicated in glucocorticoid-induced negative feedback regulation of HPA axis function (Pacak and Palkovits, 2001; Herman et al., 2002). Our data suggest that LS *Crfr2α*$^+$ neurons inhibit GABAergic targets in AHA that in turn project to PVN. If so, then LS *Crfr2*$^+$ neurons should exert a net positive-acting influence on PVN function, via a presumptive di-synaptic disinhibitory connection. To test this idea, we measured corticosterone (CORT) levels as a surrogate index of PVN activation, since the PVN positively regulates the HPA axis.

LS *Crfr2α*$^+$ neurons were optogenetically stimulated for 30 minutes, followed immediately by blood collection (Fig. 7H). Control experiments indicated that experimental handling, including anaesthetization, of animals elevates circulating CORT (data not shown), and baseline CORT was elevated in eYFP control mice, indicating that the HPA axis was activated under the testing conditions. Nevertheless, optogenetic stimulation yielded significantly higher levels of CORT in ChR2-injected mice relative to eYFP controls (Fig. 7I).

We next tested whether optogenetic inhibition of LS *Crfr2*$^+$ terminals in AHA would, conversely, reduce CORT (Fig. 7J). To maximize CORT levels, mice were subjected to IMS during photoinhibition. Although CORT levels in IMS-treated controls were similar to those in non-IMS-treated controls (Figs. 7I vs. K), reflecting the constitutive activation of the HPA axis under these conditions, optogenetic inhibition yielded a statistically significant reduction in CORT (Fig. 7K). Together, these gain- and loss-of-function data indicate that LS *Crfr2*$^+$ neurons positively modulate CORT levels in the context of an activated HPA axis. They are, therefore, consistent with the idea that these neurons exert a net positive-acting influence on PVN function.

DISCUSSION

The LS has long been implicated in the control of stress responses and anxiety, but has not previously been subjected to functional dissection of its genetically defined constituent neuronal subpopulations. Here, we have used an optogenetic approach to trace and functionally manipulate LS *Crfr2α*$^+$ neurons. We report three major findings regarding their role in anxiety. First, the valence of LS *Crfr2α*$^+$ neuronal activation is anxiogenic. Second, these effects are mediated at least in part via extra-septal projections to the AHA, rather than by an exclusively intra-septal mechanism. Lastly, transient activation of LS *Crfr2α*$^+$ neurons can induce both behavioral and neuroendocrine dimensions of a persistent anxiety state.

Crfr2 marks LS output neurons with an anxiogenic influence

The robust and dramatic ‘septal rage’ phenotype that results from certain electrolytic, physical, or chemical lesions of the septum (Spiegel et al., 1940; Brady and Nauta, 1953; Albert and Richmond, 1976) have led to a prevailing view that the output of the LS serves to dampen fear and anxiety (Sheehan et al., 2004). Anxiogenic cell populations in the LS were, therefore, inferred to act by providing local inhibition on such anxiolytic output (Henry et al., 2006). Here we identify a subpopulation of LS output neurons whose activation is anxiogenic rather than anxiolytic. This anxiogenic influence is exerted, at least in part, via

long-range inhibitory projections to the medial hypothalamus. These data argue against the long standing view that LS output serves primarily to suppress fear or anxiety in response to stressors (Sheehan et al., 2004).

Importantly, we note that our data derive from a transgenic mouse line that drives detectable Cre expression in a subset of *Crfr2* mRNA$^+$ cells. This incomplete expressivity of the transgene could reflect either stochastic variation, or expression in a deterministic subset of *Crfr2*$^+$ neurons due to incomplete capture of the entire transcriptional control region in the transgene. Whatever the explanation, the fact that complementary gain- and loss-of-function optogenetic phenotypes were observed argues that the Cre$^+$*Crfr2*$^+$ subset plays an important role in the regulation of anxiety. However, our experiments leave open the relationship of Cre$^-$, *Crfr2*$^+$ cells to anxiety.

LS *Crfr2α*$^+$ neurons act via inhibitory projections to the medial hypothalamus

Our optogenetic studies demonstrate that the anxiogenic effects of LS *Crfr2*α$^+$ neuronal activity are exerted, at least in part, via GABAergic projections to the medial hypothalamus (Fig. 1, model 2; Figs. 6E,J). These inhibitory projections exert a positive-acting influence on both the behavioral and endocrinological dimensions of a stress-induced anxious state. These effects are mediated at least in part via the inhibition of GABAergic targets within the AHA (Figs. 7L and S7A–H). These AHA target neurons innervate the PVN, a structure that regulates CORT release. Our experiments implicate LS *Crfr2α*$^+$ neurons in the regulation of circulating glucocorticoids. To our knowledge, optogenetic manipulations of specific neuronal subpopulations that lead to changes in corticosterone levels have not previously been reported. However, whether this endocrinological effect explains the persistent elevation of anxiety is unclear. Indeed, our observation that AHA targets of LS *Crfr2α*$^+$ neurons also project to the PAG raises the possibility that the behavioral and endocrinological influences of LS *Crfr2*α$^+$ neuronal activity may be mediated by parallel neural pathways, as demonstrated in the extended amygdala (LeDoux et al., 1988; Viviani et al., 2011; Kim et al., 2013).

Our data do not exclude the possibility that some LS *Crfr2*α$^+$ neurons also act intra-septally to promote anxiety, for example by inhibiting anxiolytic LS subpopulations. The existence of anxiolytic neurons is supported by the observation that excitotoxic LS lesions can enhance stress-induced activation of the HPA axis (Singewald et al., 2011). LS neurons in general are thought to send recurrent GABAergic collaterals that terminate on other neurons throughout the LS (Sheehan et al., 2004). These data suggest that the level of stress-induced anxiety may be controlled by a balance of activity between anxiogenic and anxiolytic LS populations. It has recently been shown that the BNST contains distinct anxiogenic and anxiolytic GABAergic neuronal subsets with unique patterns of long-range connections (Jennings et al., 2013; Kim et al., 2013). Whether specific anxiolytic output neurons exist in the LS, in addition to the anxiogenic outputs identified here, remains to be determined.

LS *Crfr2α*$^+$ neurons can generate persistent states of anxiety

The time-resolved nature of optogenetic manipulations has revealed that transient activation of LS *Crfr2*α$^+$ neurons can induce anxiety that persists for at least half an hour following the offset of photostimulation. Other optogenetic manipulations have revealed rapidly reversible effects on anxiety. For example, photostimulation of excitatory basolateral amygdala projections to central amygdala resulted in an acute anxiolytic effect that rapidly dissipated upon cessation of stimulation (Tye et al., 2011). Similarly, optogenetic stimulation of *Drd1a*$^+$ neurons in the oval nucleus of BNST acutely but reversibly elevated anxiety (Kim et al., 2013). In contrast, photostimulation of glutamatergic projections from ventral BNST to the ventral tegmental area (VTA) (Jennings et al., 2013) was sufficient to induce a persistent

elevation in anxiety. These results suggest that distinct pathways may be responsible for controlling acute versus persistent anxiety. It is additionally interesting to note that the two pathways thus far found to display persistence (vBNST-VTA and LS-AHA) are both anxiogenic. It remains to be seen whether persistent anxiolytic pathways exist, or if persistence is rather a unique property of circuits that elevate anxiety.

The present studies have identified a cellular point-of-entry to an important but understudied node in the brain circuitry that regulates emotional responses to stress. Our results provide further evidence of the importance of long-range GABAergic projection neurons in the control of anxiety (Jennings et al., 2013; Kim et al., 2013). Future studies should reveal the inputs to LS *Crfr2*$^{+}$ neurons, the interactions of these neurons with other genetically and functionally distinct LS subpopulations, and the functional relationship between the SHA and the extended amygdala in the control of anxiety. Together such studies should provide a neural circuit-level framework for understanding how genetic and environmental factors shape an individual's response to stress, and may identify new potential routes for therapeutic intervention in anxiety disorders.

EXPERIMENTAL PROCEDURES

Generation of *Crfr2α*-eGFPCre BAC transgenic mice

A bacterial artificial chromosome (BAC clone RP23-78P13) containing the mouse *Crfr2* gene was subjected to twp rounds of RecA-mediated homologous recombination to: 1) disrupt expression of *Inmt*, a gene present on the BAC and known to be expressed in the brain; and 2) insert an eGFPCre-SV40pA cassette at the start codon in the third exon of the brain-selective alpha-splice variant of the *Crfr2* gene. The final recombineered BAC was linearized with NotI, purified using Sepharose CL4b, confirmed by pulsed field gel electrophoresis, and then microinjected into the pronuclei of FVB/N embryos to generate transgenic mice.

Animal maintenance

The *Crfr2α*-eGFPCre BAC transgene was maintained on an FVB/N (Taconic) background. For behavior experiments, hemizygous transgenic FVB/N males were bred to nontransgenic C57BL/6N (Harlan Sprague Dawley) females, and FVBB6F1 male transgenics used for testing. Animals were housed at 23°C with *ad libitum* access to food and water in a 13-h day/11-h night cycle, with the day starting at 21:00. Behavioral testing was done during the dark cycle, starting no earlier than 11:00 and no later than 20:00. Following surgery, mice were singly housed.

Supplementary Material

Refer to Web version on PubMed Central for supplementary material.

Acknowledgments

We thank K. Deisseroth for Cre-dependent ChR2 and eNpHR AAV constructs, E. Boyden for Cre-dependent ArchT AAV construct, C. Saper for Cre-dependent hrGFP AAV construct, and L. Lo for HSV129ΔTK-TT; M. Martinez, H-J. Kim, J-S. Chang, and M. McCardle for technical help; M. Zelikowsky for statistics advice; and A. Colon, R. Bayon, R. Sauza, and J. Cochrane for animal care. This work was supported by NIH grant 5R01MH070053-10 (D.J.A.), an NIH NRSA postdoctoral fellowship grant 1F32HD055198-01 (T.E.A.), and a Beckman Fellowship (T.E.A.). D.J.A. is an HHMI investigator.

References

Adamec R, Head D, Blundell J, Burton P, Berton O. Lasting anxiogenic effects of feline predator stress in mice: sex differences in vulnerability to stress and predicting severity of anxiogenic response from the stress experience. Physiology & behavior. 2006; 88:12–29. [PubMed: 16624347]

Albert DJ, Richmond SE. Hyperreactivity and aggressiveness following infusion of local anesthetic into the lateral septum or surrounding structures. Behavioral biology. 1976; 18:211–226. [PubMed: 1033757]

Albert DJ, Wong RC. Hyperreactivity, muricide, and intraspecific aggression in the rat produced by infusion of local anesthetic into the lateral septum or surrounding areas. J Comp Physiol Psychol. 1978; 92:1062–1073. [PubMed: 573285]

Almeida-Santos AF, Gobira PH, Rosa LC, Guimaraes FS, Moreira FA, Aguiar DC. Modulation of anxiety-like behavior by the endocannabinoid 2-arachidonoylglycerol (2-AG) in the dorsolateral periaqueductal gray. Behav Brain Res. 2013; 252:10–17. [PubMed: 23714073]

Atasoy D, Aponte Y, Su HH, Sternson SM. A FLEX switch targets Channelrhodopsin-2 to multiple cell types for imaging and long-range circuit mapping. J Neurosci. 2008; 28:7025–7030. [PubMed: 18614669]

Bakshi VP, Smith-Roe S, Newman SM, Grigoriadis DE, Kalin NH. Reduction of stress-induced behavior by antagonism of corticotropin-releasing hormone 2 (CRH2) receptors in lateral septum or CRH1 receptors in amygdala. J Neurosci. 2002; 22:2926–2935. [PubMed: 11923457]

Bakshi VP, Newman SM, Smith-Roe S, Jochman KA, Kalin NH. Stimulation of lateral septum CRF2 receptors promotes anorexia and stress-like behaviors: functional homology to CRF1 receptors in basolateral amygdala. J Neurosci. 2007; 27:10568–10577. [PubMed: 17898228]

Bale TL, Vale WW. CRF and CRF receptors: role in stress responsivity and other behaviors. Annu Rev Pharmacol Toxicol. 2004; 44:525–557. [PubMed: 14744257]

Bandler R, Shipley MT. Columnar organization in the midbrain periaqueductal gray: modules for emotional expression? Trends in neurosciences. 1994; 17:379–389. [PubMed: 7817403]

Biag J, Huang Y, Gou L, Hintiryan H, Askarinam A, Hahn JD, Toga AW, Dong HW. Cyto- and chemoarchitecture of the hypothalamic paraventricular nucleus in the C57BL/6J male mouse: a study of immunostaining and multiple fluorescent tract tracing. J Comp Neurol. 2012; 520:6–33. [PubMed: 21674499]

Brady JV, Nauta WJ. Subcortical mechanisms in emotional behavior: affective changes following septal forebrain lesions in the albino rat. J Comp Physiol Psychol. 1953; 46:339–346. [PubMed: 13109048]

Davis M, Walker DL, Miles L, Grillon C. Phasic vs sustained fear in rats and humans: role of the extended amygdala in fear vs anxiety. Neuropsychopharmacology : official publication of the American College of Neuropsychopharmacology. 2010; 35:105–135. [PubMed: 19693004]

Debanne D, Boudkkazi S, Campanac E, Cudmore RH, Giraud P, Fronzaroli-Molinieres L, Carlier E, Caillard O. Paired-recordings from synaptically coupled cortical and hippocampal neurons in acute and cultured brain slices. Nat Protoc. 2008; 3:1559–1568. [PubMed: 18802437]

Drugan RC, Skolnick P, Paul SM, Crawley JN. Low doses of muscimol produce anticonflict actions in the lateral septum of the rat. Neuropharmacology. 1986; 25:203–205. [PubMed: 3703171]

Feder A, Nestler EJ, Charney DS. Psychobiology and molecular genetics of resilience. Nat Rev Neurosci. 2009; 10:446–457. [PubMed: 19455174]

Felix-Ortiz AC, Beyeler A, Seo C, Leppla CA, Wildes CP, Tye KM. BLA to vHPC Inputs Modulate Anxiety-Related Behaviors. Neuron. 2013; 79:658–664. [PubMed: 23972595]

Gagneten S, Le Y, Miller J, Sauer B. Brief expression of a GFP cre fusion gene in embryonic stem cells allows rapid retrieval of site-specific genomic deletions. Nucleic acids research. 1997; 25:3326–3331. [PubMed: 9241248]

Gradinaru V, Thompson KR, Deisseroth K. eNpHR: a Natronomonas halorhodopsin enhanced for optogenetic applications. Brain Cell Biol. 2008; 36:129–139. [PubMed: 18677566]

Gray, JA.; McNaughton, N. The Neuropsychology of Anxiety. 2. New York: Oxford University Press; 2000.

Gross C, Hen R. The developmental origins of anxiety. Nat Rev Neurosci. 2004; 5:545–552. [PubMed: 15208696]

Han X, Chow BY, Zhou H, Klapoetke NC, Chuong A, Rajimehr R, Yang A, Baratta MV, Winkle J, Desimone R, et al. A high-light sensitivity optical neural silencer: development and application to optogenetic control of non-human primate cortex. Front Syst Neurosci. 2011; 5:18. [PubMed: 21811444]

Henke PG. Hippocampal pathway to the amygdala and stress ulcer development. Brain Res Bull. 1990; 25:691–695. [PubMed: 2289157]

Henry B, Vale W, Markou A. The effect of lateral septum corticotropin-releasing factor receptor 2 activation on anxiety is modulated by stress. J Neurosci. 2006; 26:9142–9152. [PubMed: 16957071]

Herman JP, Cullinan WE, Ziegler DR, Tasker JG. Role of the paraventricular nucleus microenvironment in stress integration. Eur J Neurosci. 2002; 16:381–385. [PubMed: 12193178]

Jennings JH, Sparta DR, Stamatakis AM, Ung RL, Pleil KE, Kash TL, Stuber GD. Distinct extended amygdala circuits for divergent motivational states. Nature. 2013; 496:224–228. [PubMed: 23515155]

Kheirbek MA, Drew LJ, Burghardt NS, Costantini DO, Tannenholz L, Ahmari SE, Zeng H, Fenton AA, Hen R. Differential control of learning and anxiety along the dorsoventral axis of the dentate gyrus. Neuron. 2013; 77:955–968. [PubMed: 23473324]

Kim SY, Adhikari A, Lee SY, Marshel JH, Kim CK, Mallory CS, Lo M, Pak S, Mattis J, Lim BK, et al. Diverging neural pathways assemble a behavioural state from separable features in anxiety. Nature. 2013; 496:219–223. [PubMed: 23515158]

Kjelstrup KG, Tuvnes FA, Steffenach HA, Murison R, Moser EI, Moser MB. Reduced fear expression after lesions of the ventral hippocampus. Proc Natl Acad Sci U S A. 2002; 99:10825–10830. [PubMed: 12149439]

LeDoux JE, Iwata J, Cicchetti P, Reis DJ. Different projections of the central amygdaloid nucleus mediate autonomic and behavioral correlates of conditioned fear. J Neurosci. 1988; 8:2517–2529. [PubMed: 2854842]

Liu J, Yu B, Neugebauer V, Grigoriadis DE, Rivier J, Vale WW, Shinnick-Gallagher P, Gallagher JP. Corticotropin-releasing factor and Urocortin I modulate excitatory glutamatergic synaptic transmission. J Neurosci. 2004; 24:4020–4029. [PubMed: 15102917]

Liu J, Yu B, Orozco-Cabal L, Grigoriadis DE, Rivier J, Vale WW, Shinnick-Gallagher P, Gallagher JP. Chronic cocaine administration switches corticotropin-releasing factor2 receptor-mediated depression to facilitation of glutamatergic transmission in the lateral septum. J Neurosci. 2005; 25:577–583. [PubMed: 15659593]

Lo L, Anderson DJ. A Cre-dependent, anterograde transsynaptic viral tracer for mapping output pathways of genetically marked neurons. Neuron. 2011; 72:938–950. [PubMed: 22196330]

Lupien SJ, McEwen BS, Gunnar MR, Heim C. Effects of stress throughout the lifespan on the brain, behaviour and cognition. Nat Rev Neurosci. 2009; 10:434–445. [PubMed: 19401723]

Madisen L, Zwingman TA, Sunkin SM, Oh SW, Zariwala HA, Gu H, Ng LL, Palmiter RD, Hawrylycz MJ, Jones AR, et al. A robust and high-throughput Cre reporting and characterization system for the whole mouse brain. Nat Neurosci. 2010; 13:133–140. [PubMed: 20023653]

Mahan AL, Ressler KJ. Fear conditioning, synaptic plasticity and the amygdala: implications for posttraumatic stress disorder. Trends in neurosciences. 2012; 35:24–35. [PubMed: 21798604]

Mongeau R, Miller GA, Chiang E, Anderson DJ. Neural correlates of competing fear behaviors evoked by an innately aversive stimulus. J Neurosci. 2003; 23:3855–3868. [PubMed: 12736356]

Nieh EH, Kim SY, Namburi P, Tye KM. Optogenetic dissection of neural circuits underlying emotional valence and motivated behaviors. Brain research. 2012; 1511:73–92. [PubMed: 23142759]

Pacak K, Palkovits M. Stressor specificity of central neuroendocrine responses: implications for stress-related disorders. Endocr Rev. 2001; 22:502–548. [PubMed: 11493581]

Petreanu L, Huber D, Sobczyk A, Svoboda K. Channelrhodopsin-2-assisted circuit mapping of long-range callosal projections. Nat Neurosci. 2007; 10:663–668. [PubMed: 17435752]

Radulovic J, Ruhmann A, Liepold T, Spiess J. Modulation of learning and anxiety by corticotropin-releasing factor (CRF) and stress: differential roles of CRF receptors 1 and 2. J Neurosci. 1999; 19:5016–5025. [PubMed: 10366634]

Risold PY, Swanson LW. Structural evidence for functional domains in the rat hippocampus. Science. 1996; 272:1484–1486. [PubMed: 8633241]

Risold PY, Swanson LW. Chemoarchitecture of the rat lateral septal nucleus. Brain Res Brain Res Rev. 1997a; 24:91–113. [PubMed: 9385453]

Risold PY, Swanson LW. Connections of the rat lateral septal complex. Brain Res Brain Res Rev. 1997b; 24:115–195. [PubMed: 9385454]

Sartor GC, Aston-Jones GS. A septal-hypothalamic pathway drives orexin neurons, which is necessary for conditioned cocaine preference. J Neurosci. 2012; 32:4623–4631. [PubMed: 22457508]

Sheehan TP, Chambers RA, Russell DS. Regulation of affect by the lateral septum: implications for neuropsychiatry. Brain Res Brain Res Rev. 2004; 46:71–117. [PubMed: 15297155]

Singewald GM, Rjabokon A, Singewald N, Ebner K. The modulatory role of the lateral septum on neuroendocrine and behavioral stress responses. Neuropsychopharmacology : official publication of the American College of Neuropsychopharmacology. 2011; 36:793–804. [PubMed: 21160468]

Sparks, PD.; LeDoux, JE. The Septal Complex as Seen Through the Context of Fear. In: Numan, R., editor. The Behavioral Neuroscience of the Septal Region. New York: Springer-Verlag; 2000. p. 234-269.

Spiegel EA, Miller HR, Oppenheimer MJ. Forebrain and rage reactions. J Neurophysiol. 1940; 3:538–548.

Thomas E, Strickland CE, Yadin E, Burock DA. Effects of chlordiazepoxide on single-unit activity in the septal region of the freely moving rat: aversive vs. non-aversive contexts. Pharmacol Biochem Behav. 2005; 80:151–159. [PubMed: 15652391]

Thomas E, Burock D, Knudsen K, Deterding E, Yadin E. Single unit activity in the lateral septum and central nucleus of the amygdala in the elevated plus-maze: a model of exposure therapy? Neuroscience letters. 2013; 548:269–274. [PubMed: 23769728]

Treit D, Pesold C. Septal lesions inhibit fear reactions in two animal models of anxiolytic drug action. Physiology & behavior. 1990; 47:365–371. [PubMed: 1970655]

Tye KM, Prakash R, Kim SY, Fenno LE, Grosenick L, Zarabi H, Thompson KR, Gradinaru V, Ramakrishnan C, Deisseroth K. Amygdala circuitry mediating reversible and bidirectional control of anxiety. Nature. 2011; 471:358–362. [PubMed: 21389985]

Tye KM, Deisseroth K. Optogenetic investigation of neural circuits underlying brain disease in animal models. Nat Rev Neurosci. 2012; 13:251–266. [PubMed: 22430017]

Ulrich-Lai YM, Herman JP. Neural regulation of endocrine and autonomic stress responses. Nat Rev Neurosci. 2009; 10:397–409. [PubMed: 19469025]

Viviani D, Charlet A, van den Burg E, Robinet C, Hurni N, Abatis M, Magara F, Stoop R. Oxytocin selectively gates fear responses through distinct outputs from the central amygdala. Science. 2011; 333:104–107. [PubMed: 21719680]

Research highlights

- *Crfr2* defines a molecularly distinct subset of predominantly GABAergic LS neurons
- *Crfr2*$^{+}$ neuronal activation promotes, while inhibition suppresses, persistent anxiety
- These anxiogenic effects are exerted in part via projections to medial hypothalamus
- LS *Crfr2*$^{+}$ outputs positively regulate circulating corticosteroid levels

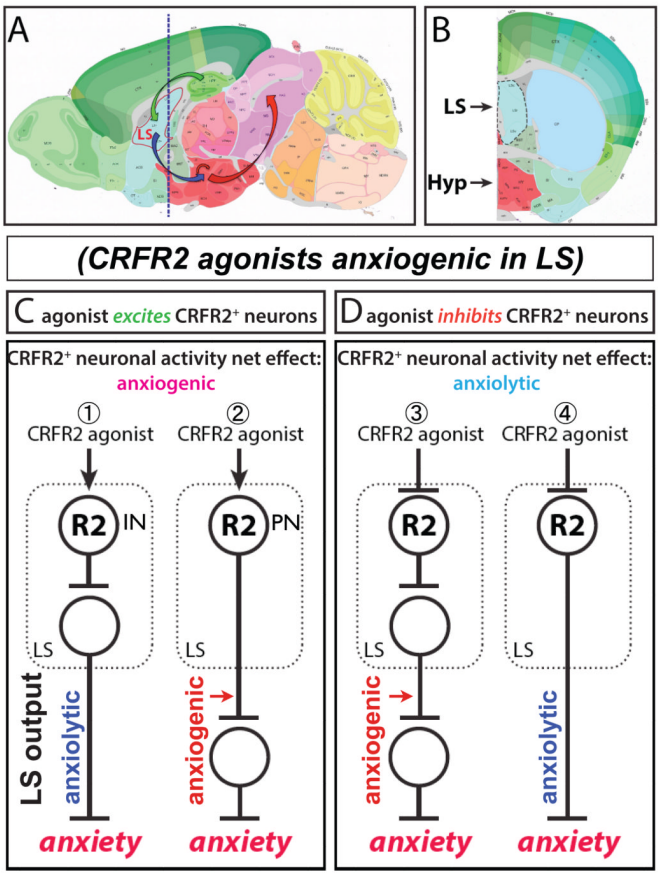

Figure 1. Circuit models for LS CRFR2$^+$ neuronal regulation of anxiety

(A) Sagittal plane of LS anatomy showing simplified feedforward connections. (B) Coronal section at plane indicated by dashed line in (A). Modified from Allen Brain Atlas (www.brain-map.org). (C, D) Circuit models consistent with known anxiogenic effect of CRFR2 agonists in the LS. Depending on whether agonists excite (C) or inhibit (D) CRFR2$^+$ ("R2") neurons, increased R2 neuronal activity would be anxiogenic (C) or anxiolytic (D). GABAergic R2 neurons (Fig. 2F) may be local interneurons ("IN;" C1, D3) or projection neurons ("PN;" C2, D4). LS output may be anxiolytic (C1, D4) or anxiogenic (C2, D3).

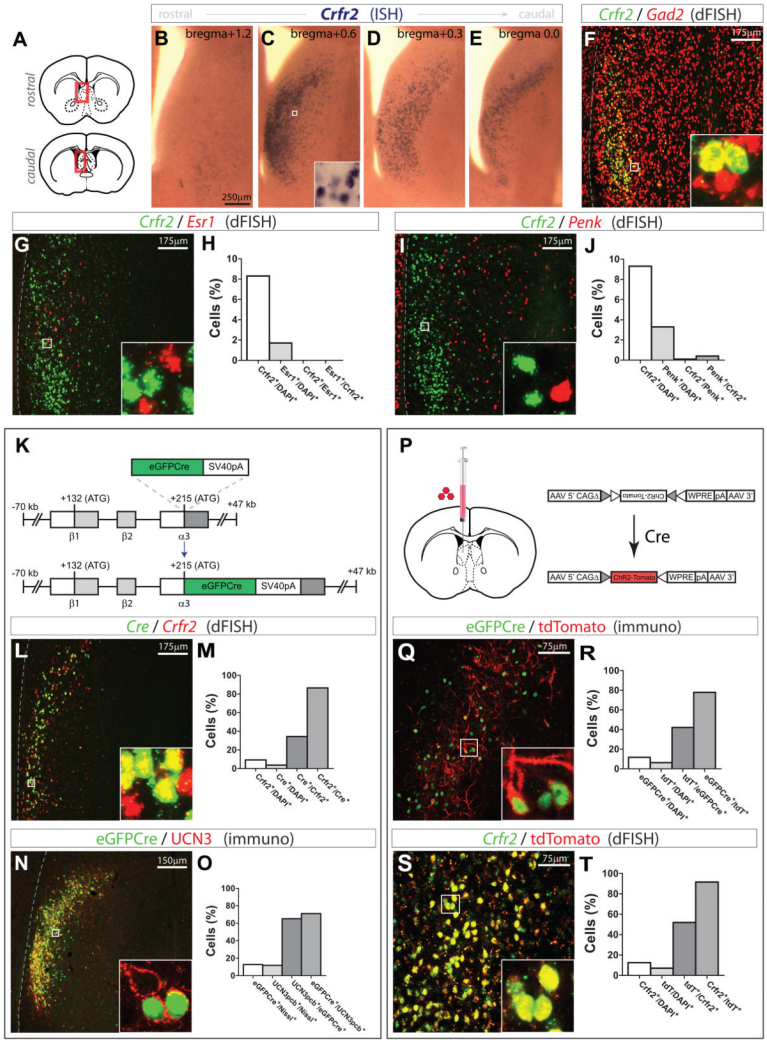

Figure 2. Characterization and transgenic targeting of LS *Crfr2α*$^+$ neurons

(A–E) *Crfr2* mRNA ISH; coronal diagrams in (A) depict region analyzed.

(F) dFISH for *Crfr2* (green) and *Gad2* (red).

(G,H) dFISH for *Crfr2* (green) vs *Esr1* (red): *Crfr2*$^+$/DAPI$^+$ = 8.3%, *Esr1*$^+$/DAPI$^+$ = 1.7%, *Crfr2*$^+$/*Esr1*$^+$ = 0, *Esr1*$^+$/*Crfr2*$^+$ = 0; total *n* = 11,086 DAPI$^+$ cells

(I,J) dFISH for *Crfr2* (green) vs *Penk* (red): *Crfr2*$^+$/DAPI$^+$ = 9.3%, *Penk*$^+$/DAPI$^+$ = 3.3%, *Crfr2*$^+$/*Penk*$^+$ = 0.1%, *Penk*$^+$/*Crfr2*$^+$ = 0.4%; total *n* = 8,274 DAPI$^+$ cells

(K) *Crfr2α*-eGFPCre BAC transgene design.

(L,M) dFISH, Cre mRNA (green) vs. *Crfr2* mRNA (red): *Crfr2*$^+$/DAPI$^+$ = 9.3%, Cre$^+$/DAPI$^+$ = 3.7%, Cre$^+$/*Crfr2*$^+$ = 34.4%, *Crfr2*$^+$/Cre$^+$ = 86.6%; total *n* = 17,537 DAPI$^+$ cells

(N,O) eGFPCre$^+$ nuclei (green) vs. UCN3 pericellular baskets (pcbs; red); counts from areas with detectable transgene expression. UCN3$^+$ pcbs colocalize with synaptophysin (data not shown). eGFPCre$^+$/DAPI$^+$ = 12.8%, UCN3pcb$^+$/DAPI$^+$ = 11.8%, UCN3pcb$^+$/eGFPCre$^+$ = 65.2%, eGFPCre$^+$/UCN3pcb$^+$ = 71.0%; total *n* = 2,665 Nissl$^+$ cells

(P) Injection site (left) and Cre-dependent AAV (right).

(Q,R) Transgenic eGFPCre$^+$ nuclei (green) vs. recombined, viral tdT (red); counts from areas containing tdT$^+$ cells. eGFPCre$^+$/DAPI$^+$ = 11.7%, tdT$^+$/DAPI$^+$ = 6.3%, tdT$^+$/eGFPCre$^+$ = 42.1%, eGFPCre$^+$/tdT$^+$ = 77.9%; total *n* = 3,586 DAPI$^+$ cells

(S,T) dFISH for *Crfr2* mRNA (green) vs. tdT mRNA (red); counts from areas containing tdT^+ cells. $Crfr2^+/DAPI^+$ = 12.5%, $tdT^+/DAPI^+$ = 7.1%, $tdT^+/Crfr2^+$ = 51.9%, $Crfr2^+/tdT^+$ = 91.6%; total n = 5,829 $DAPI^+$ cells

In this and subsequent figures, dashed lines at left indicate lateral ventricle (LV), boxed regions shown at higher magnification in insets.

See also Figures S1 and S2.

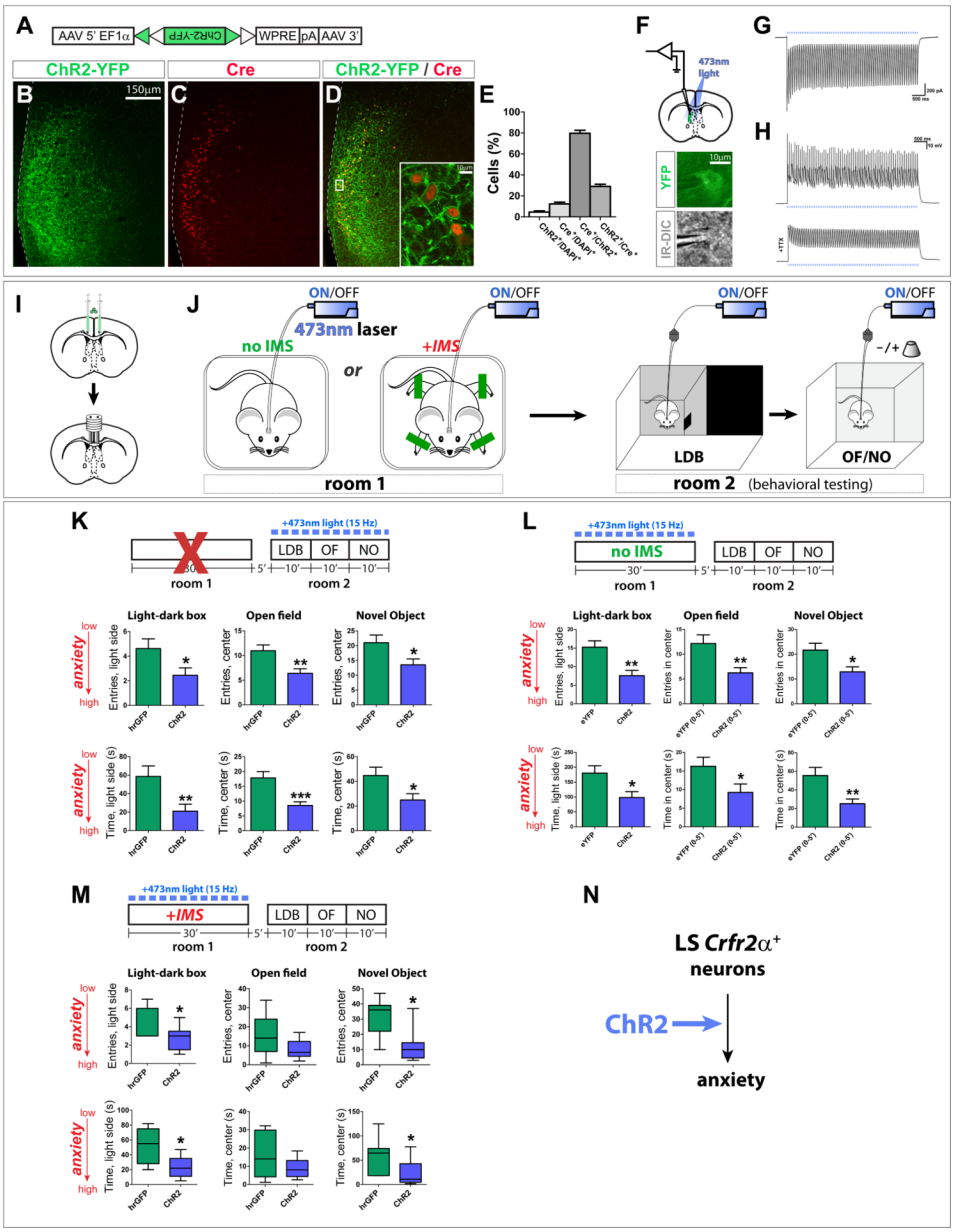

Figure 3. Optogenetic stimulation of LS *Crfr2α*$^+$ neurons induces a persistent, anxious state

(A) Cre-dependent ChR2-YFP AAV.

(B–D) Injection of (A) into *Crhr2*α-eGFPCre LS yielded ChR2-YFP (green) in Cre$^+$ cells (red).

(E) Recombination specificity and sensitivity; counts done in areas containing ChR2-YFP$^+$ cells: ChR2$^+$/DAPI$^+$ = 4.6±1.1%, Cre$^+$/DAPI$^+$ = 12.4±1.7%, Cre$^+$/ChR2$^+$=79.7±2.9%, ChR2$^+$/Cre$^+$=29.0±2.1% (mean±s.e.m.). Total *n* = 9,673 DAPI$^+$ cells from 2 mice.

(F) *top*, ChR2 activity in *Crfr2α*$^+$ cells assessed in acute slices; *bottom*, patched YFP$^+$ neuron under infrared differential interference contrast (IR-DIC) microscopy.

(G,H) Robust photocurrents were observed (G) that were sufficient to drive repetitive, tetrodotoxin(TTX)-sensitive spiking in ChR2-YFP$^+$ neurons (H).

(I,J) Surgical manipulations and behavioral testing.

(K) Photostimulation of *Crfr2a*$^+$ neurons during behavioral testing increased anxiety. hrGFP(*n*=39) vs. ChR2(*n*=38): LDB, entries in light side (4.6±0.8 vs. 2.5±0.6, *P*<0.05), time in light side (58.6±11.4 vs. 21.0±7.6, *P*<0.01); OF, entries in center (11.0±1.2 vs 6.4±0.9, *P*<0.01), time in center (17.9±2.1 vs. 8.5±1.2, *P*<0.001); NO, entries in center (21.0±2.6 vs. 13.6±2.0, *P*<0.05), time in center (44.7±6.8 vs. 24.9±5.1, *P*<0.05). *P* values represent two-tailed unpaired t-tests. Values indicate mean±s.e.m.
(L) Photostimulation of *Crfr2a*$^+$ neurons increased anxiety during subsequent testing. eYFP(*n*=13) vs. ChR2(*n*=12): LDB, entries in light side (15.2±1.7 vs. 7.6±1.4, *P*<0.01), time in light side (180.2±24.8 vs. 98.0±20.1, *P*<0.05); OF(0–5′), entries in center (12.2±1.8 vs. 6.3±1.0, *P*<0.01), time in center (16.3±2.4 vs. 9.2±2.3, *P*<0.01); NO(0–5′), entries in center (21.7±2.8 vs. 13.0±2.0, *P*<0.05), time in center (55.4±8.7 vs. 25.3±5.0, *P*<0.01).
(M) Stimulating *Crfr2a*$^+$ neurons exacerbates the anxiogenic effects of IMS (mice were habituated to minimize ceiling effect confound, see methods). hrGFP (*n*=7) vs. ChR2 (*n*=8), data presented as Mann-Whitney *U* value, *P* value: LDB, entries in light side (*U* = 7.5, *P*<0.05), time in light side (*U* = 10.5, *P*<0.05); OF, entries in center (*U* = 15.5, *P*>0.15), time in center (*U* = 22.5, *P*>0.55); NO, entries in center (*U* = 7.0, *P*<0.05), time in center (*U* = 10.0, *P*<0.05).
(N) Model of LS *Crfr2a*$^+$ neuronal valence based on optogenetic stimulation.
See also Figure S3.

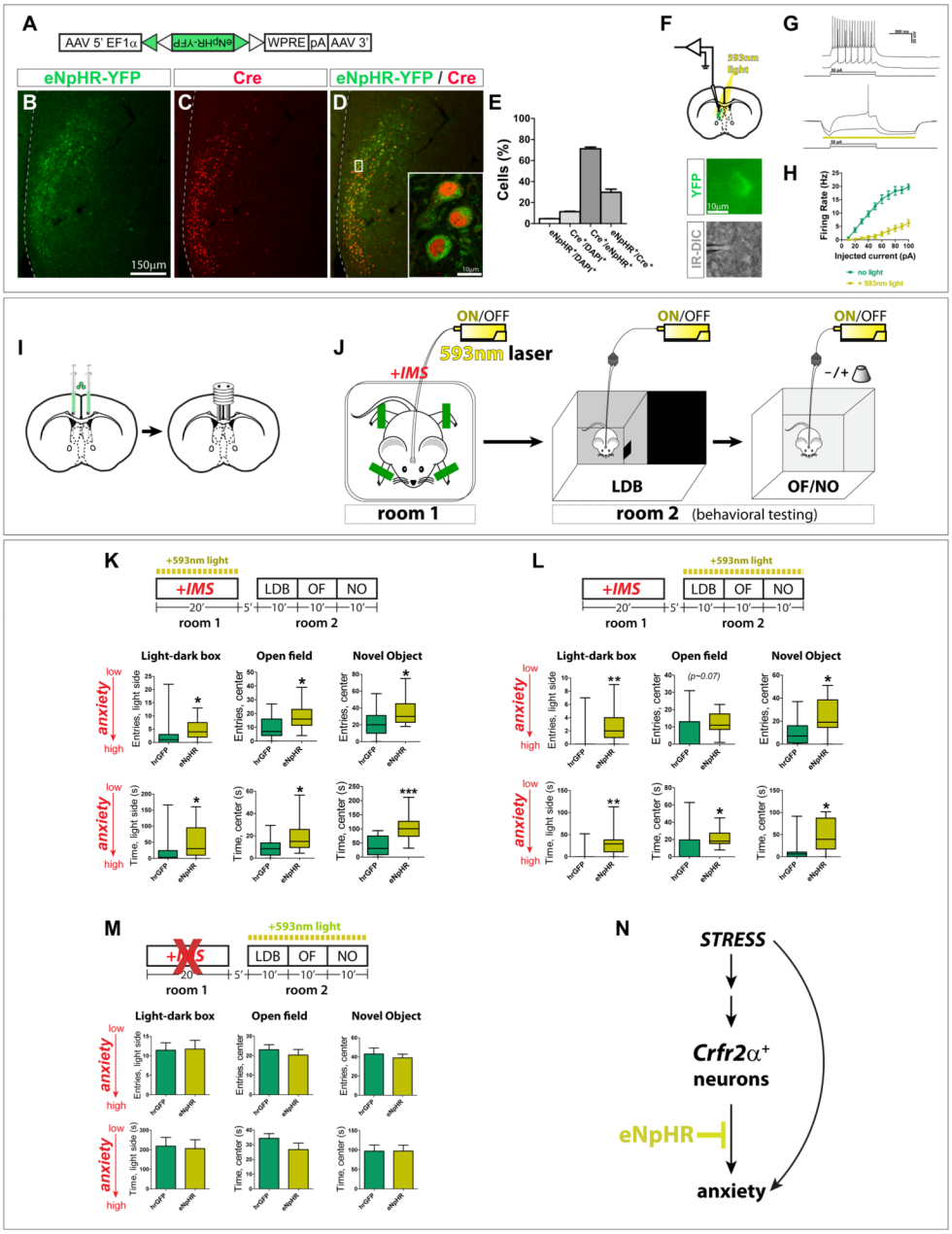

Figure 4. LS *Crfr2α*$^+$ neurons are necessary for the induction and expression of a stress-induced, anxiogenic state

(A) Cre-dependent eNpHR(2.0)-YFP AAV.

(B–D) Injection of (A) into *Crhr2*α-eGFPCre LS yielded eNpHR-YFP (green) in Cre$^+$ cells (red).

(E) Recombination specificity and sensitivity; counts from areas containing eNpHR-YFP$^+$ cells: eNpHR$^+$/DAPI$^+$ = 4.7±0.2%, Cre$^+$/DAPI$^+$ = 11.4±0.4%, Cre$^+$/eNpHR$^+$=71.2±1.6%, eNpHR$^+$/Cre$^+$=29.8±3.0% (mean±s.e.m.). Total n = 8,216 DAPI$^+$ cells from 2 mice.

(F–H) Recordings from eNpHR-YFP$^+$*Crfr2α*$^+$ neurons. (G) Cell in response to the same current injections in absence (*top*) or presence (*bottom*) of 593nm light. (H) 593nm light significantly suppressed firing of eNpHR-YFP$^+$ neurons ($F_{1,108}$ = 28.69, P<0.001).

(I,J) Surgical manipulations and behavioral testing.

(K) Photoinhibition of *Crfr2a*$^{+}$ neurons only during IMS reduced anxiety in subsequent testing. hrGFP (*n*=15) vs. eNpHR (*n*=17), data presented Mann-Whitney *U* value, *P* value: LDB, entries in light side (*U* = 64.0, *P*<0.05), time in light side (*U* = 62.5, *P*<0.05); OF, entries in center (*U* = 69.0, *P*<0.05), time in center (*U* = 64.5, *P*<0.05); NO, entries in center (*U* = 73.5, *P*<0.05), time in center (*U* = 34.0, *P*<0.001).
(L) IMS mice that received photoinhibition of *Crfr2a*$^{+}$ neurons only during behavioral testing showed reduced anxiety relative to controls. hrGFP (*n*=11) vs. eNpHR (*n*=11): LDB, entries in light side (*U* = 21.5, *P*<0.01), time in light side (*U* = 20.0, *P*<0.01); OF, entries in center (*U* = 25.5, *P*=0.07), time in center (*U* = 23.0, *P*<0.05); NO, entries in center (*U* = 22.0, *P*<0.05), time in center (*U* = 21.0, *P*<0.05).
(M) Inhibiting *Crfr2a*$^{+}$ neurons in the absence of IMS does not alter anxiety. hrGFP(n=11) vs. eNpHR (*n*=11): LDB, entries in light side (11.5±1.9 vs. 11.7±2.3, *P*>0.9), time in light side (218.7±44.6 vs. 206.4±45.2, *P*>0.8); OF, entries in center (23.1±2.6 vs. 20.4±2.8, *P*>0.45), time in center (34.4±3.2 vs. 26.7±4.4, *P*>0.15); NO, entries in center (43.0±6.3 vs. 39.0±3.9, *P*>0.6), time in center (97.0±15.8 vs. 97.5±14.9, *P*>0.95).
(N) Model for LS *Crfr2a*$^{+}$ neuronal valence based on optogenetic inhibition.
See also Figure S4.

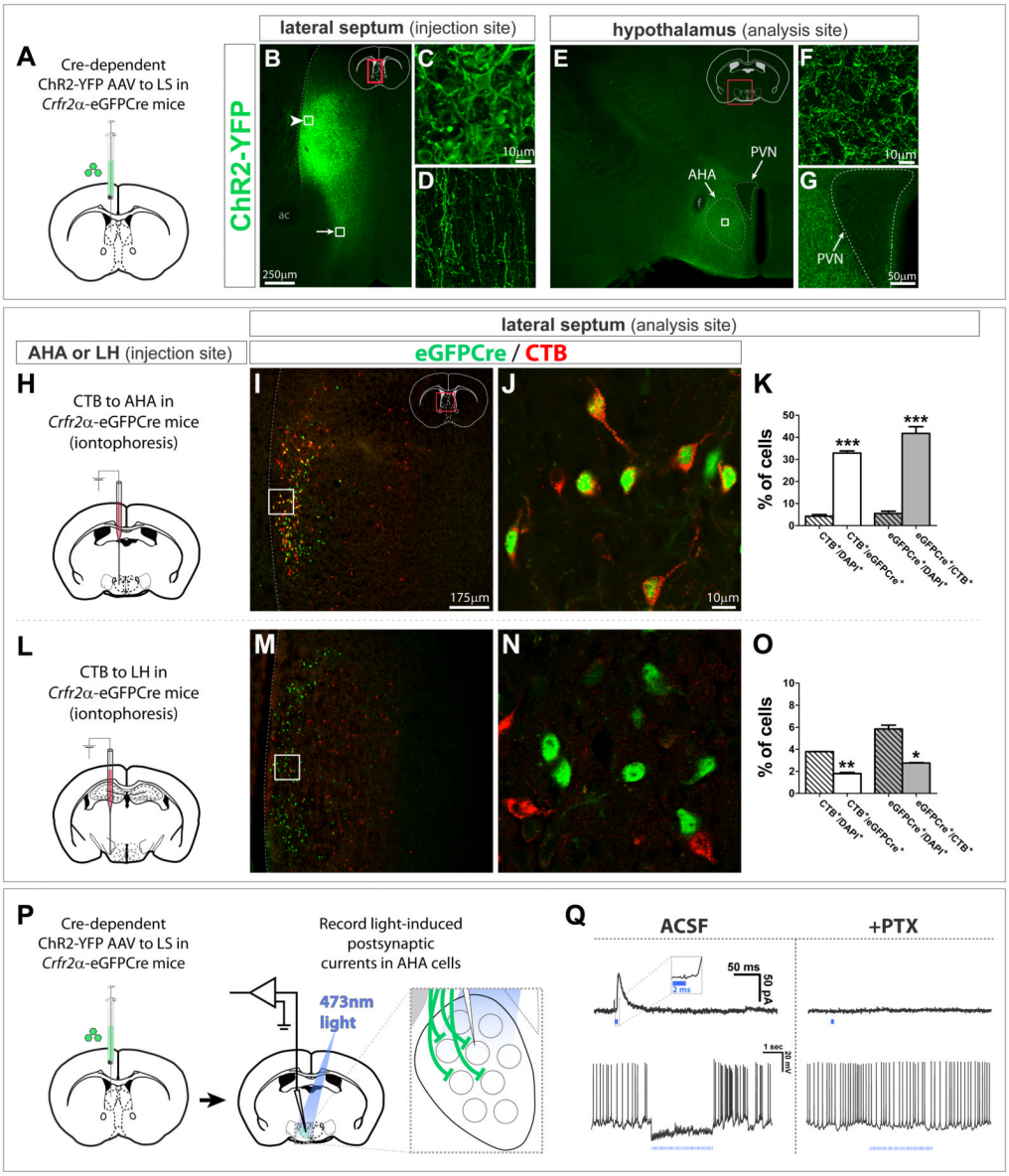

Figure 5. LS *Crfr2α*$^+$ neurons make GABAergic synapses in the AHA

(A–G) Cre-dependent ChR2-YFP AAV injected into *Crfr2*α-eGFPCre LS labeled cell bodies (arrowhead in B, enlarged in C) and axons (arrow in B, enlarged in D) Terminals were densest in AHA (E). All AHA labeling was axonal (F, enlarged from boxed area in E). YFP$^+$ axons appeared to be excluded from the PVN (G). ac, anterior commissure; f, fornix; PVN, paraventricular hypothalamic nucleus.

(H–O) CTB retrograde tracing. eGFPCre (green) and CTB (red) in the LS of *Crfr2α*-eGFPCre mice that received iontophoretic injection of CTB into the AHA (I,J) or LH (M,N). (K) A significant fraction of *Crfr2α*$^+$ neurons project to AHA (CTB$^+$/DAPI$^+$ = 4.3±0.7% vs. CTB$^+$/eGFPCre$^+$ = 33.0±1.0%, P<0.001), and *Crfr2α*$^+$ neurons comprise a large fraction of the neurons that project to AHA from middle levels of LS (GFPCre$^+$/DAPI$^+$ = 5.5±1.1% vs. eGFPCre$^+$/CTB$^+$ = 42.0±3.1%, P<0.001). (O) Few *Crfr2*α$^+$ neurons innervate the LH (CTB$^+$/DAPI$^+$ = 3.8±0.01% vs. CTB$^+$/eGFPCre$^+$ = 1.8±0.1%, P<0.01), with most projections to this region coming from *Crfr2α*$^-$ cells (GFPCre$^+$/DAPI$^+$ = 5.9±0.4% vs.

eGFPCre$^+$/CTB$^+$ = 2.8±0.1%, P<0.05). Counts done at bregma+0.6 in LS regions that contained CTB$^+$ cells. Total n = 7,737 DAPI$^+$ cells (AHA) and n = 5,767 DAPI$^+$ cells (LH). Values indicate mean±s.e.m.

(P,Q) CRACM in standard ACSF or plus 100μM picrotoxin (PTX). (Q) Single 2ms pulses of 473nm light evoked IPSCs blocked by PTX (*top*). Inset, higher temporal resolution to illustrate response latency. (*bottom*), picrotoxin-sensitive inhibition of spontaneous firing observed by presynaptic terminal photostimulation (15Hz, 2ms pulses).

See also Figure S5.

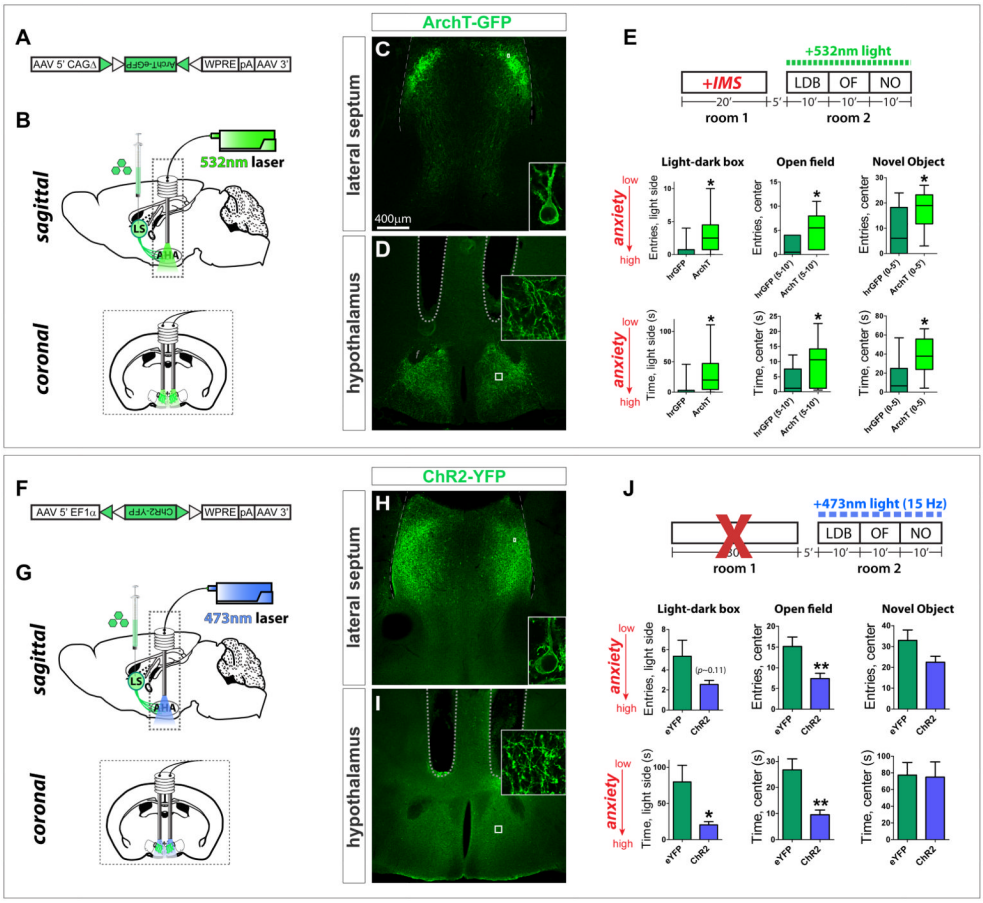

Figure 6. LS *Crfr2a*$^+$ projections to AHA are necessary for stress-induced anxiety

(A) Cre-dependent ArchT-GFP AAV.

(B–E) Axon terminal inhibition. (C,D) ArchT-GFP in LS *Crfr2a*$^+$ (C) cell bodies and (D) and axons in AHA. (E) Photoinhibition of *Crfr2a*$^+$ axon terminals in AHA during behavioral testing in IMS-stressed mice reduces anxiety. hrGFP (*n*=10) vs. ArchT (*n*=12), data presented Mann-Whitney *U* value, *P* value: LDB, entries in light side (*U* = 25.0, *P*<0.05), time in light side (*U* = 24.0, *P*<0.05); OF(5–10′), entries in center (*U* = 21.5, *P*<0.05), time in center (*U* = 26.0, *P*<0.05); NO(0–5′), entries in center (*U* = 29.5, *P*<0.05), time in center (*U* = 19.0, *P*<0.05).

(F) Cre-dependent ChR2-YFP AAV.

(G–J) Axon terminal stimulation. (H,I) ChR2-YFP in LS *Crfr2a*$^+$ (H) cell bodies and (I) axons. (J) Stimulation of *Crfr2a*$^+$ axon terminals in AHA during testing increased anxiety. eYFP(*n*=17) vs. ChR2(*n*=15): LDB, entries in light side (5.2±1.6 vs. 2.5±0.4, *P*>0.1), time in light side (79.9±23.2 vs. 20.3±4.6, *P*<0.05); OF, entries in center (15.1±2.3 vs. 7.4±1.3, *P*<0.01), time in center (26.8±4.2 vs. 9.5±1.8, *P*<0.01); NO, entries in center (32.9±5.0 vs. 22.5±2.9, *P*=0.08), time in center (77.2±15.2 vs. 74.9±18.3, *P*>0.1); values indicate mean ±s.e.m. *P* values represent two-tailed unpaired t-tests.

Dashed lines in (D,I) indicate guide tips.

See also Figure S6.

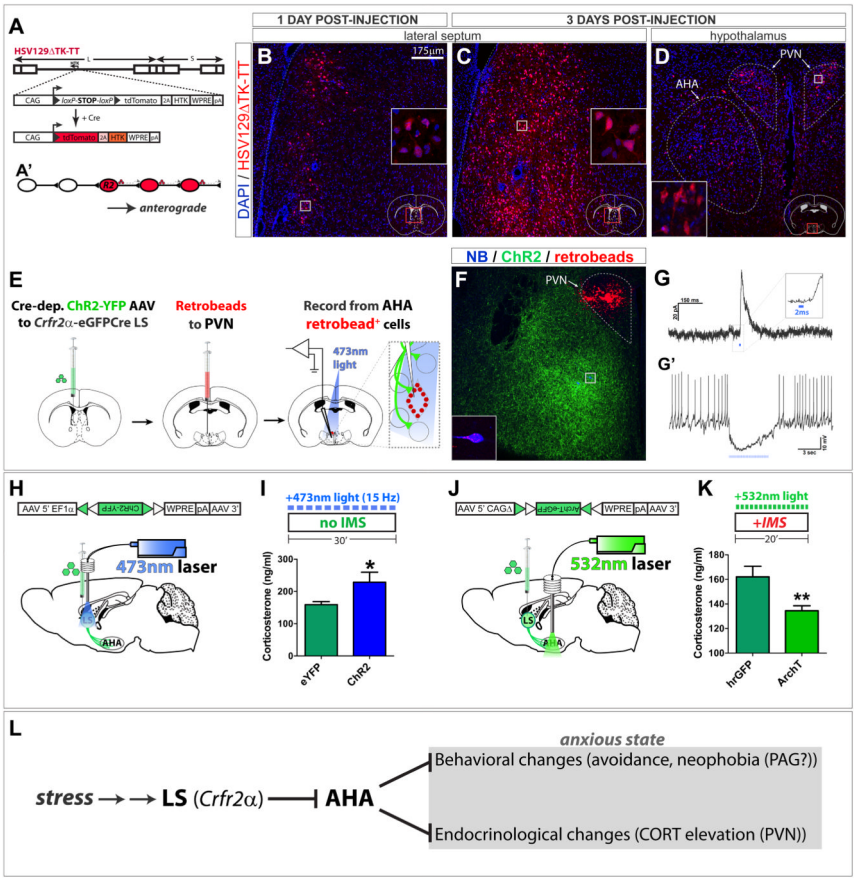

Figure 7. LS *Crfr2α*$^+$ projections to AHA are polysynaptically upstream of PVN and positively regulate corticosterone levels

(A,A′) HSV129ΔTK-TT.

(B–D) tdT (red) in HSV129ΔTK-TT-injected *Crfr2α*-eGFPCre mice counterstained with DAPI (blue) at 1 (B) or 3 (C,D) days post-injection (dpi) in LS (B,C) or medial hypothalamus (D). Dashed lines in (D) demarcate PVN (upper right) and AHA (lower left).

(E–G) Combined CRACM and retrograde tracing. (F) A slice used for recording; *Crfr2*α$^+$ChR2-YFP$^+$ axons originating from LS (green), retrobeads (red), and two neurobiotin-filled neurons (blue). The cell that yielded the traces in (G) is shown at higher magnification in the inset. (G) A 2ms pulse of 473nm light induced monosynaptic IPSCs in 4/9 retrobead$^+$ AHA neurons that were sufficient to inhibit firing (G′).

(H,I) Optogenetic stimulation of LS *Crfr2α*$^+$ neurons increased CORT. eYFP(*n*=9) vs. ChR2(*n*=9): CORT, ng/ml (159.2±9.3 vs. 228.8±30.9, *P*<0.05).

(J,K) Optogenetic inhibition of LS *Crfr2*α$^+$ projections to AHA decreased CORT. hrGFP(*n*=15) vs. ArchT-GFP(*n*=17): CORT, ng/ml (162.1±8.6 vs. 134.5±4.1, *P*<0.01). Values indicate mean±s.e.m.

(L) Proposed model for LS *Crfr2*α$^+$ neuronal control of stress-induced anxiety.

See also Figure S7.